Journal of Zhejiang University-SCIENCE B (Biomedicine & Biotechnology) 2025 26(8):789-804
www.jzus.zju.edu.cn; www.springer.com/journal/11585
E-mail: jzus_b@zju.edu.cn

Research Article
https://doi.org/10.1631/jzus.B2400242

Potential effect of endothelial progenitor cells on pentylenetetrazole-induced seizures in rats: an evaluation of relevant lncRNAs

Shimaa O. ALI[1]✉, Nancy N. SHAHIN[1], Marwa M. SAFAR[2,3], Sherine M. RIZK[1]

[1]*Biochemistry Department, Faculty of Pharmacy, Cairo University, Cairo 11562, Egypt*
[2]*Pharmacology and Toxicology Department, Faculty of Pharmacy, Cairo University, Cairo 11562, Egypt*
[3]*Pharmacology and Biochemistry Department, Faculty of Pharmacy, The British University in Egypt, Cairo 11837, Egypt*

Abstract: Objective: The use of stem cells is a promising strategy for seizure treatment owing to their unique characteristics. We investigated the role of endothelial progenitor cells (EPCs) in a pentylenetetrazole (PTZ)-induced rat seizure model. A selected panel of long noncoding RNAs (lncRNAs), which maintain an elaborate balance in brain neural regulatory networks as well as the autophagy pathway, was also targeted. Methods: The impact of intravenously administered EPCs on PTZ-induced kindling in rats was evaluated by measuring the expression of neuronal damage markers, neurotrophic factors, and relevant lncRNA genes. Rat behavior was assessed using Y-maze test and open field test (OFT). Results: EPCs mitigated seizure-associated neurological damage and reversed PTZ-induced working memory and locomotor activity deficits, as evidenced by improved performance in the Y-maze test and OFT. EPC treatment reversed the downregulation of the expression of the lncRNAs *Evf2*, *Pnky*, *Dlx1*, *APF*, *HOTAIR*, and *FLJ11812*. EPCs also boosted vascular endothelial growth factor (VEGF) expression. The ameliorative effect achieved by EPCs was comparable to that produced by valproate. Conclusions: These findings indicate that EPCs ameliorate kindling epileptic seizures and their associated abnormalities and that the effect of EPCs may be mediated via the upregulation of certain regulatory lncRNAs.

Key words: Endothelial progenitor cell (EPC); Long noncoding RNA (lncRNA); Pentylenetetrazole (PTZ); Neuronal damage; Seizure

1 Introduction

Epilepsy is a neurological disorder that arises due to excessive firing of excitatory neurons in a specific region of the brain. In fact, the existing evidence suggests that chronic epilepsy and intermittent seizures are related to neuronal damage and responsive alterations in the human hippocampus. Elevated cerebrospinal fluid and blood levels of neuron-specific enolase, soluble protein-100B (S100B), neurofilament heavy chain protein (NEFH), heat shock protein 70 (HSP70), and ubiquitin carboxy-terminal hydrolase L1 (UCH-L1) are associated with neuronal damage and enhanced blood–brain barrier (BBB) permeability (Dunn et al., 2021; Kim et al., 2022; Li et al., 2022). Additionally, BBB impairment plays an integral role in ictogenesis, epileptogenesis, and persistence of seizures (Gu et al., 2020; van Vliet et al., 2020).

Long noncoding RNAs (lncRNAs) represent one of the greatest portions of the mammalian noncoding transcriptome and have been implicated in numerous functions, including posttranscriptional regulation, chromatin modulation, and protein-complex configuration. They are generally essential for development, differentiation, and metabolism (Fernandes et al., 2019; Zhang et al., 2019). During primate nervous system development, thousands of new lncRNAs emerge and are expressed in a profoundly region-specific manner (Cuevas-Diaz Duran et al., 2019; Li et al., 2021). LncRNAs are also critical regulators of autophagy (Ma et al., 2022), and increasing evidence shows that lncRNAs modulate the autophagy process by interacting with RNA-binding proteins and downregulating the induction of microRNAs (Wang et al., 2015). However, the relationship between autophagy and

✉ Shimaa O. ALI, shimaa.omar@pharma.cu.edu.eg
Shimaa O. ALI, https://orcid.org/0000-0003-0855-5580

Received May 10, 2024; Revision accepted Sept. 20, 2024; Crosschecked Aug. 6, 2025

lncRNAs has still not been fully elucidated (Wang PH et al., 2023).

Although epilepsy can be effectively treated, in most cases, the treatment gap (the number of individuals who need treatment but do not receive it) is massive, especially in the developing world, because antiepileptic drugs (AEDs) are either inaccessible or too expensive. Nevertheless, not all epileptic patients respond to existing medical treatments. There is increasing evidence that surgery, neurostimulation, and diet can be valuable (Hogan, 2018; Kobayashi et al., 2020). As we reported in a previous study, endothelial progenitor cells (EPCs) ameliorate seizure-associated alterations through the upregulation of autophagy (Ali et al., 2019). However, a prospective correlation between epileptic seizures and lncRNAs that regulate cerebral function and autophagy in animal models is understudied. The goal of this study was to investigate the possible impacts of EPCs on certain lncRNA signatures in a model of pentylenetetrazole (PTZ)-induced seizures.

2 Materials and methods

2.1 Animals

The study involved 60 adult male Wistar rats ((170±30) g) purchased from the National Cancer Institute (Cairo, Egypt). The animals were housed in standard plastic cages under strict temperature control ((23±1) ℃) and humidity ((60±10)%) with a 12-h light/dark cycle. The rats were allowed to receive standard chow and water ad libitum. Before any experimental manipulation, the rats were given a one-week initial period of adaptation.

2.2 Chemicals

PTZ was obtained from Sigma-Aldrich Chemical Co. (St. Louis, MO, USA), and valproic acid (VPA) was obtained from Sanofi-Aventis (France). Other reagents used were of pure analytical grade.

2.3 Isolation, culture, and labeling of EPCs

The procedures are described in detail in our previous work (Ali et al., 2019). In brief, bone marrow was extracted from the femurs and tibias of male syngeneic Fisher-344 rats (150–200 g). Mononuclear cells were isolated using density-gradient centrifugation at 400*g* for 30 min. Thereafter, the cells were suspended in culture medium consisting of 20% (0.2 g/mL) fetal bovine serum, 50 μg/mL streptomycin, 50 U/mL penicillin, 2 mmol/L glutamine, 5 ng/mL basic fibroblast growth factor, and 50 ng/mL vascular endothelial growth factor (VEGF). These cells were then cultured in fibronectin-coated flasks and incubated in 5% CO_2 for 7 d at 37 ℃ to obtain EPCs. The culture medium was replaced every 48 h. Following two washes in serum-free medium, the EPCs were collected and suspended in PKH26 solution, a stable red fluorochrome, and then administered intravenously into the rats' tail veins. PKH26-labeled cells are ideal for in vivo tracking.

2.4 Experimental design

The rats were arbitrarily divided into four groups (15 rats/group). The first group consisted of normal rats that received vehicle only (normal control). The second group comprised rats that were given 35 mg/kg PTZ three times/week, administered nine times intraperitoneally, resulting in three consecutive generalized convulsions (Stage 5 on Racine's scale (Racine, 1972)) (PTZ group, kindled rats). The dose of PTZ used was based on previous studies (Dhir, 2012; Erkeç, 2015; Pahwa and Goel, 2016). PTZ is preferred because it has no special neurotoxic effects; therefore, it is an ideal model for researching the relationship between the onset of seizures and neuronal damage. Additionally, the mortality rate is low, and the majority of animals experience generalized seizures (Erkeç, 2015). The third group comprised kindled rats that, after experiencing the first generalized convulsion, received a single dose of EPCs (2×10^6 cells) injected intravenously via the tail vein (Safar et al., 2016; Ali et al., 2019) (the EPC group). The final group included kindled rats that were orally administered VPA (150 mg/kg), a standard AED, 30 min before each PTZ injection (Croce et al., 2014) (the VPA group).

2.5 Characterization and fluorescence imaging of EPCs

Flow cytometric immunophenotyping was used to identify the EPCs' clusters of differentiation (CD31, CD34, and CD133). The rat hippocampi were also imaged using a fluorescence microscope to confirm the homing of the PKH26-labeled injected cells, as described in our previous paper (Ali et al., 2019).

2.6 Seizure severity score

Each animal was positioned in the middle of a 30 cm×30 cm×50 cm cage immediately following the PTZ injection, and its behavior was observed for 30 min. Seizure severity was classified into six stages according to Racine (1972): 0 for no reaction or immobility; 1 for shivering; 2 for light clonic seizure; 3 for whole- or partial-body continuous clonic seizure while maintaining posture; 4 for severe clonic seizure (whole-body severe seizing, animal on the verge of falling over); and 5 for tonic-clonic seizure with loss of balance and/or jumping.

2.7 Neurobehavioral assessment

2.7.1 Y-maze spontaneous alternation test

We used the Y-maze test to assess working memory and exploratory activity. The apparatus had three matching arms (A, B, and C; 40.0 cm×4.5 cm×12.0 cm, 120° apart). Each rat was placed in the middle of the apparatus, and during a 5-min observation period, the number of entries into each arm was recorded. A successful alternation occurred when the rat entered a new arm consecutively before returning to the two previously visited arms (Ghafouri et al., 2016). Same-arm return (SAR) scores were documented. The total numbers of alternations and arm entries were also recorded, and to calculate the spontaneous alternation percentage (SAP), the total number of alternations was divided by the total number of possible alternations. The total number of possible alternations was obtained by subtracting 2 from the total number of arm entries, and the result was multiplied by 100 to obtain the percentage value.

2.7.2 Open field test (OFT)

Locomotor activity was measured using an open-field apparatus (113 cm×113 cm×44 cm). We positioned each rat in the bottom right corner of the test apparatus and videotaped it for 3 min with a camera 100 cm away from the arena. Every time the rat moved all four paws from one grid square to another, it crossed a single line, and this incident was documented to estimate the ambulation frequency. Latency time, grooming (a consistent pattern of quick foreleg motions toward the face or body for cleaning), and rearing (the frequency of rats standing on their hind limbs) were also measured (Zimcikova et al., 2017).

2.8 Sampling

At the end of the experimental period, the rats were sacrificed by decapitation under light anesthesia. Blood was collected in heparin-containing tubes and centrifuged at 1000*g* for 15 min at 4 ℃ within 30 min of collection for plasma separation. Aliquots of the separated plasma were stored at −80 ℃ for subsequent evaluation of the following brain damage markers: S100B, NEFH, HSP70, and UCH-L1. In addition, other aliquots of the separated plasma were used for gene expression analysis of the lncRNAs *Evf2*, *Pnky*, *Dlx1*, *APF*, *HOTAIR*, and *FLJ11812*.

Brain samples were dissected from individual groups and preserved in 10% (volume fraction) buffered formalin saline. The specimens were further subjected to immunohistochemical characterization of VEGF.

2.9 Determination of plasma S100B, NEFH, HSP70, and UCH-L1 levels

S100B, HSP70, NEFH, and UCH-L1 were quantified via enzyme-linked immunosorbent assay (ELISA) kits supplied by Cusabio Biotech Co. (Catalog Nos. CSB-E08066r and CSB-E08308r, Wuhan, China), MyBioSource (Catalog No. MBS7269972, San Diego, USA), and the BioassayTech Laboratory (Catalog No. E2312Ra, Shanghai, China), respectively. The procedures were performed as specified by the manufacturer's protocol.

2.10 Determination of plasma mRNA expression levels of the lncRNAs *Evf2*, *Pnky*, *Dlx1*, *APF*, *HOTAIR*, and *FLJ11812* by RT-qPCR

2.10.1 RNA extraction

Total RNA was isolated from plasma by means of an RNA extraction kit supplied by Qiagen (Venlo, the Netherlands). The isolated RNA was then eluted with RNase-free water and decontaminated using a Thermo Scientific Gene JET RNA purification kit (Hemel Hempstead, UK). A NanoDrop 2000 spectrophotometer, set at a detection wavelength of 260 nm (Thermo Fisher Scientific, Waltham, USA), was used to determine the concentration.

2.10.2 cDNA synthesis and qPCR

2.10.2.1 Step one: reverse transcription (RT)

Complementary DNA (cDNA) was produced from RNA using a high-capacity cDNA RT kit (Applied Biosystems, CA, USA). The reaction was conducted as directed by the manufacturer using 10 μL of RNA sample. The reaction mixture was then incubated in an Applied Biosystems 9800 Fast Thermal Cycler. The thermal cycler was set to operate for the following durations: 10 min at 25 ℃, 120 min at 37 ℃, and 5 s at 85 ℃. For later analysis, the prepared cDNA was then stored at −70 ℃.

2.10.2.2 Step two: quantitative polymerase chain reaction (qPCR)

An Applied Biosystems kit was used, which provided premixed SYBR Green PCR master mix. The PCR mixture consisted of SYBR Green PCR master mix (25 μL), template cDNA (5 μL), forward primer (0.5 μL), reverse primer (0.5 μL), and deionized water (19 μL). The reaction mixture was then incubated in an Applied Biosystems 9800 Fast Thermal Cycler. The following conditions were used in the thermal cycler: a primary hold at 95 ℃ for 10 min, and then 45 cycles of 3 min at 95 ℃, 30 s at 95 ℃, and 1 min of annealing/extension. The temperature range for annealing was 56–60 ℃. The primer sequences are shown in Table 1. Additionally, we constructed an amplification curve with real-time PCR system software and determined the C_T values for each lncRNA. The internal control used to normalize the C_T values was glyceraldehyde-3-phosphate dehydrogenase (*GAPDH*), and the $\Delta\Delta C_T$ method was utilized to calculate the changes in target gene expression, which were then displayed as the fold changes ($FC=2^{-\Delta\Delta C_T}$).

Table 1 Sequences of the RT-qPCR primers

Gene	Primer sequence
Evf2	Forward: 5'-CTCCCTCCGCTCAGTATAGATTTC-3'
	Reverse: 5'-CCTCCCCGGTGAATATCTCTT-3'
Pnky	Forward: 5'-GCAGGAGTTGCTGCACTACA-3'
	Reverse: 5'-GTACCGCTGAATAACGCCCT-3'
Dlx1	Forward: 5'-AGAGAGGACCAATGAGCCTT-3'
	Reverse: 5'-CACGGTGGATTTCAATCGGT-3'
APF	Forward: 5'-CTCCTCTATATTGTGTTCAAG-3'
	Reverse: 5'-GTGTTCATAAGGTAACCTGAA-3'
HOTAIR	Forward: 5'-GGGGCTTCCTTGCTCTTCTTATC-3'
	Reverse: 5'-GGTAGAAAAAGCAACCACGAAGC-3'
FLJ11812	Forward: 5'-GCAGTTTCAC CTAAAGAGCA GC-3'
	Reverse: 5'-TTCCTTCCCA CCTCCACCC-3'
GAPDH	Forward: 5'-CTCCCATTCTTCCACCTTTG-3'
	Reverse: 5'-CTTGCTCTCAGTATCCTTGC-3'

RT-qPCR: reverse transcription-quantitative polymerase chain reaction; GAPDH: glyceraldehyde-3-phosphate dehydrogenase.

2.11 Immunohistochemical detection of hippocampal VEGF

Briefly, microwave antigen retrieval of deparaffinized sections was performed for 5 min before quenching peroxidase activity with 3% (0.03 g/mL) H_2O_2 in phosphate-buffered saline (PBS) for 15 min. The tissue slides were rehydrated and incubated at 4 ℃ with primary VEGF antibodies (Catalog No. AAM51, Serotec, Düsseldorf, Germany; diluted 1:1000 (volume ratio)) overnight. Following a PBS wash, the slides were blocked for endogenous peroxidases using H_2O_2 for 30 min at room temperature. The sections were then incubated for 30 min with a biotinylated secondary antibody before being stained with 3,3'-diaminobenzidine (DAB) solution using a DAB-substrate kit (Mouse/Rabbit ImmunoDetector DAB HRP Kit, BioSB, USA). Finally, we counterstained the slides for 2–3 min with hematoxylin before they were examined via a digital video camera mounted on a Leica DMLB2 light microscope (Leica Microsystems, Germany). For high-power fields (200×), CellSens dimensions software (Olympus Software, Tokyo, Japan) was used to quantify positive expression as an area percentage (10 fields, frame 20 μm). During the immunohistochemical analysis, investigators who were blinded to the sample code handled the samples.

2.12 Statistical analysis

We used the Shapiro-Wilk test to determine whether the data were normally distributed. The data are expressed as the mean and standard error of the mean (SEM). To test for differences between groups, we used one-way analysis of variance (ANOVA); then, we performed the Tukey-Kramer post hoc multiple comparisons test. The OFT (grooming, rearing, and ambulation frequency parameters) and the Y-maze test data are expressed as medians (25th and 75th percentiles). The nonparametric Kruskal-Wallis test was used to analyze these data, and Dunn's post hoc test

was used for multiple comparisons. Variable associations were investigated using Spearman's correlation and linear regression analyses. GraphPad Prism Version 8.0.1 (GraphPad® Software, San Diego, California, USA) was used for all statistical analyses. $P<0.05$ was considered to indicate statistical significance.

3 Results

3.1 Effects of EPCs on the seizure severity score

PTZ injection caused the quick induction of different stages of seizures from Stage 0 to major tonic-clonic convulsions. The control animals did not exhibit any seizure behavior; thus, their mean seizure score was 0. Compared with the seizure scores of rats in the control group, the scores were significantly greater in the PTZ group but lower in the EPC group. Significantly, EPCs resulted in an improvement of this score relative to VPA (starting from the fourth injection of PTZ) (Fig. 1).

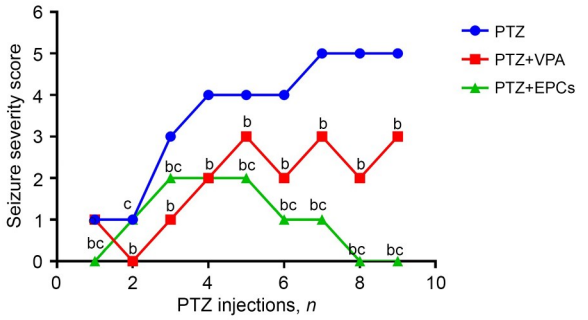

Fig. 1 Seizure severity score. The values are represented as medians. [b] Significantly different from the PTZ group; [c] Significantly different from the PTZ+VPA group. $P<0.05$ is considered to indicate statistical significance. The data were analyzed using the Kruskal-Wallis test followed by Dunn's multiple comparisons test. EPCs: endothelial progenitor cells; PTZ: pentylenetetrazole; VPA: valproic acid.

3.2 Effects of EPCs on PTZ-induced alterations in neurobehavioral function

Working memory impairment is one of the hallmarks of epileptic seizures. Working memory was significantly reduced after PTZ administration, as measured by the Y-maze spontaneous alternation test. The SAP and total arm entries were significantly lower in the PTZ group than in the control group, whereas the SAR values were significantly greater. EPCs significantly reduced the SAR score and increased the SAP and total number of arm entries in rats compared with the PTZ and PTZ+VPA groups (Figs. 2a–2c).

In the OFT, all epileptic rats demonstrated motor impairment. The latency time varied significantly between the groups, with the PTZ group exhibiting a significantly longer latency than the control, EPC, and VPA groups. This effect was greater in the EPC group than in the VPA group (Fig. 2d). The frequencies of grooming, rearing, and ambulation were significantly lower in the PTZ group than in the control group. Furthermore, rats exposed to EPCs had significantly higher grooming and rearing rates, as well as a greater frequency of ambulation, than those in either the PTZ or VPA group (Figs. 2e–2g).

3.3 Effects of EPCs on PTZ-induced changes in plasma levels of neuronal damage markers

As shown in Fig. 3a, the plasma S100B level significantly increased (by 2-fold) in the PTZ group compared with the control group. Compared with PTZ treatment, EPC and VPA treatments resulted in significant reductions in plasma S100B levels by 59% and 47%, respectively. It is noteworthy that EPCs produced a significantly greater effect than VPA.

Epileptic rats exhibited a 2.4-fold increase in the plasma NEFH concentration compared with control rats. On the other hand, EPCs and VPA significantly lowered NEFH levels by 52% and 27%, respectively, compared with the PTZ group, with EPCs showing a much greater effect (Fig. 3b). Rats with PTZ-induced seizures had significantly greater plasma HSP70 concentrations than control rats, specifically 188% greater. Compared with the PTZ treatment, the EPC and VPA treatments resulted in significant reductions of almost 40% and 50%, respectively (Fig. 3c).

Similarly, the plasma UCH-L1 concentration was significantly greater in epileptic rats than in control rats, reaching almost 2.2-fold the normal control value. Compared with PTZ, the administration of EPCs and VPA significantly reduced the plasma UCH-L1 concentration by 34% and 19%, respectively; however, their effects were not significantly different from each other (Fig. 3d).

3.4 Effects of EPCs on PTZ-induced changes in mRNA expression levels of the lncRNAs *Evf2*, *Pnky*, *Dlx1*, *APF*, *HOTAIR*, and *FLJ11812*

As demonstrated in Fig. 4, there was a prominent drop in the messenger RNA (mRNA) expression of the

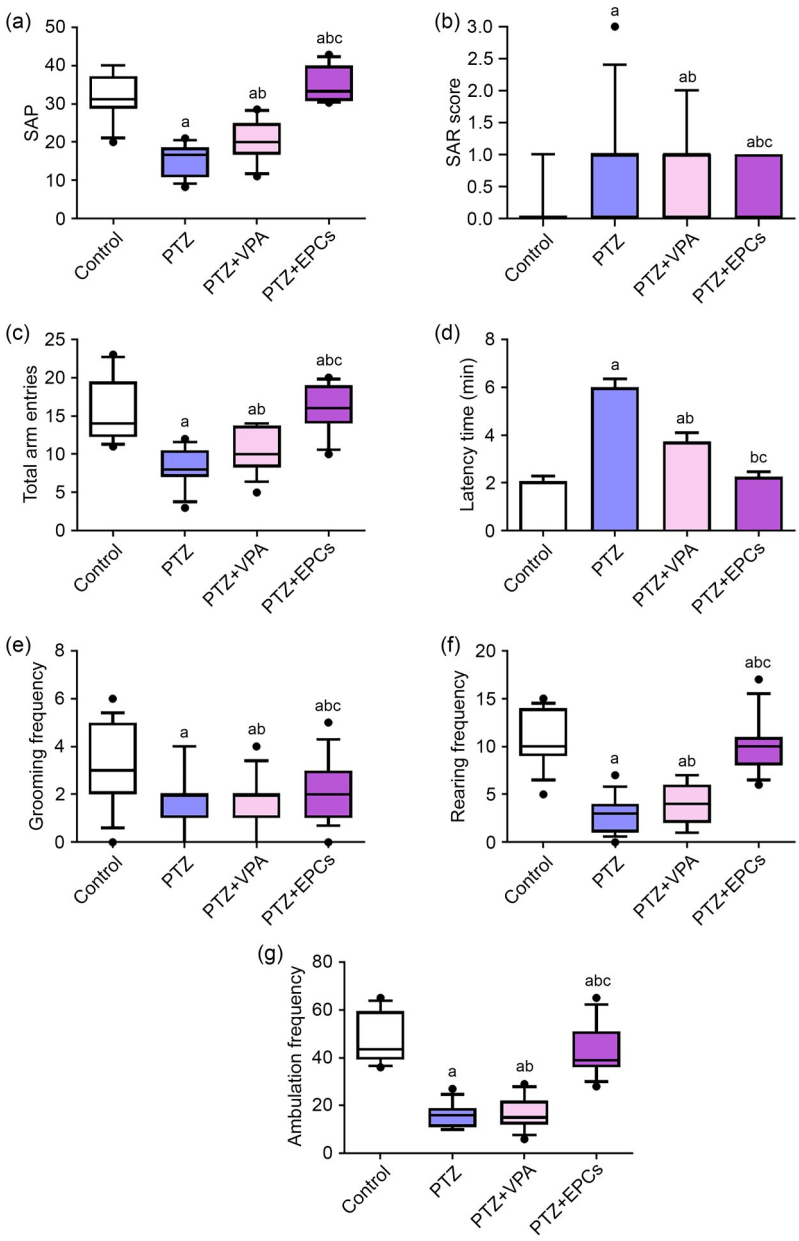

Fig. 2 Effects of EPCs on PTZ-induced alterations in neurobehavioral function: Y-maze spontaneous alternation test (a–c) and OFT (d–g). Within the box plots of SAP (a), SAR scores (b), total arm entries (c), grooming frequency (e), rearing frequency (f), and ambulation frequency (g), each horizontal line represents the median and the boxes represent the intervals between the 25th and 75th percentiles. The whiskers symbolize the intervals between the 10th and 90th percentiles. Data points outside the 10th and 90th percentiles are represented by filled circles. The Kruskal-Wallis test was used to analyze these parameters, followed by Dunn's post hoc test for multiple comparisons, except for the latency time (d), which was analyzed using one-way ANOVA followed by the Tukey-Kramer test, with each column with a vertical line representing the mean±SEM (n=13). [a] Significantly different from the control group; [b] Significantly different from the PTZ group; [c] Significantly different from the PTZ+VPA group. P<0.05 is considered to indicate statistical significance. ANOVA: analysis of variance; EPCs: endothelial progenitor cells; OFT: open field test; PTZ: pentylenetetrazole; SAP: spontaneous alternation percentage; SAR: same-arm return; SEM: standard error of the mean; VPA: valproic acid.

lncRNAs *Evf2*, *Pnky*, *APF*, *HOTAIR*, and *FLJ11812* in the PTZ group compared with the control group, with values of 70%, 85%, 84%, 83%, and 50%, respectively. In contrast, there was a tendency toward a decrease in the lncRNA *Dlx1* expression, which was not statistically significant.

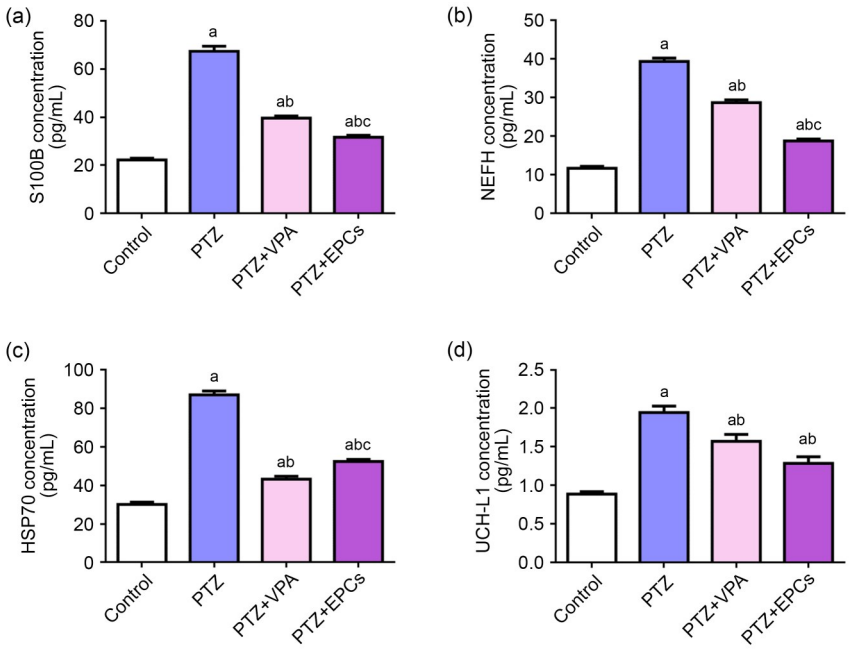

Fig. 3 Effects of EPCs on PTZ-induced changes in the plasma levels of neuronal damage markers: S100B (a), NEFH (b), HSP70 (c), and UCH-L1 (d). The data were analyzed using one-way ANOVA followed by the Tukey-Kramer test. Each column with a vertical line represents the mean±SEM (n=10). [a] Significantly different from the control group; [b] Significantly different from the PTZ group; [c] Significantly different from the PTZ+VPA group. Significance is considered to be at P<0.05. ANOVA: analysis of variance; EPCs: endothelial progenitor cells; NEFH: neurofilament heavy chain protein; HSP70: heat shock protein 70; PTZ: pentylenetetrazole; S100B: soluble protein-100B; SEM: standard error of the mean; UCH-L1: ubiquitin carboxy-terminal hydrolase L1; VPA: valproic acid.

Compared with those in the PTZ group, the mRNA expression levels of the lncRNAs *Evf2*, *Pnky*, *Dlx1*, *APF*, *HOTAIR*, and *FLJ11812* in the EPC group were significantly increased, by nearly 6-, 42-, 9-, 28-, 19-, and 2-fold, respectively. These increases were substantially greater than those in the VPA group. Interestingly, treatment with EPCs increased the expression levels of *Evf2*, *Pnky*, *Dlx1*, *APF*, *HOTAIR*, and *FLJ11812* by 1.0-, 5.0-, 3.0-, 3.0-, 2.5-, and 0.3-fold, respectively, in comparison with those in the control group.

A similar increasing trend was observed for VPA, yet was only exhibited significantly in the expression levels of the lncRNAs *Pnky*, *APF*, and *HOTAIR* relative to the PTZ group; however, VPA caused smaller elevations than EPCs, resulting in 10-, 12-, and 12-fold greater increases, respectively, compared with the PTZ group. Remarkably, the VPA group exhibited significant reductions in the expression of the lncRNAs *Evf2* and *FLJ11812* and no change in the lncRNA *Dlx1* expression level compared with the control group.

3.5 Effects of EPCs on PTZ-induced alterations in immunohistochemically detected expression of hippocampal VEGF

PTZ administration significantly decreased the level of VEGF in the hippocampal region by 64% in comparison with that in the control group, as measured by the percentage of immunostained area (Fig. 5). On the other hand, compared with the PTZ group, the level of VEGF in the EPC group significantly increased to 232%, thus effectively normalizing VEGF expression. Notably, the outcome achieved by EPCs was remarkably more pronounced than that achieved by the standard AED.

3.6 Correlation analysis

Spearman's correlation matrix revealed significant linear correlations between brain- and autophagy-specific lncRNAs, neuronal damage markers, and VEGF (Fig. 6a; Table S1). Spearman's correlation analysis of all samples simultaneously revealed that the lncRNA *Dlx1* was positively associated with the lncRNAs *Evf2* (r=0.5504, P=0.005 32; Fig. 6b) and

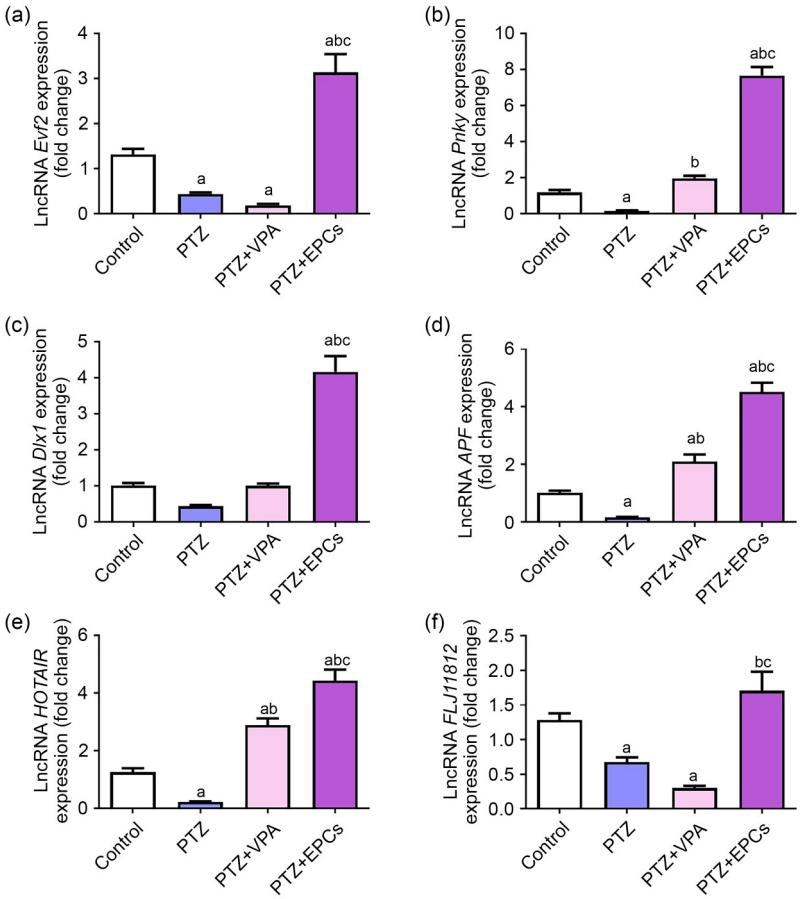

Fig. 4 Effects of EPCs on PTZ-induced changes in the expression levels of lncRNAs, namely, *Evf2* (a), *Pnky* (b), *Dlx1* (c), *APF* (d), *HOTAIR* (e), and *FLJ11812* (f). The data were analyzed using one-way ANOVA followed by the Tukey-Kramer test. Each column with a vertical line represents the mean±SEM (n=6). [a] Significantly different from the control group; [b] Significantly different from the PTZ group; [c] Significantly different from the PTZ+VPA group. Significance is considered to be at P<0.05. ANOVA: analysis of variance; EPCs: endothelial progenitor cells; LncRNA: long noncoding RNA; PTZ: pentylenetetrazole; SEM: standard error of the mean; VPA: valproic acid.

HOTAIR (r=0.8530, P<0.000 01; Fig. 6c). Moreover, the lncRNA *HOTAIR* was significantly associated with both the lncRNAs *Pnky* and *APF* (r=0.9017, P<0.000 01; r=0.9261, P<0.000 01, respectively; Figs. 6d and 6e), as well as UCH-L1 (r=0.4704, P=0.020 34; Fig. 6f). On the other hand, there were strong negative associations between VEGF and the lncRNAs *HOTAIR* (r=−0.4730, P=0.019 57; Fig. 6g) and *Pnky* (r=−0.5478, P=0.005 59; Fig. 6h).

4 Discussion

Epileptic seizures are clearly connected with brain damage and neuronal loss. The epileptic cerebrovasculature is strongly affected by BBB impairment. BBB damage has been observed in the brain tissue of patients with drug-resistant epilepsy, as well as in epileptic rat models (Morin-Brureau et al., 2011; Yamanaka et al., 2021). It is reasonable to suppose that in epileptic brains, a vicious cycle develops whereby BBB damage enables the occurrence of seizures and enduring seizure activity aggravates BBB injury and further promotes seizures. Seizures have a significant impact on the neurovascular system. This pathological neurovascular ramification could interrupt the energy supply, increase cellular damage, and slow energy-demanding homeostatic processes such as the active transport required for neuronal repolarization. Collectively, these changes ultimately prolong depolarization and delay seizure termination (Marchi and Lerner-Natoli, 2013).

The hippocampus has long been known for its involvement in memory and learning. Hippocampal

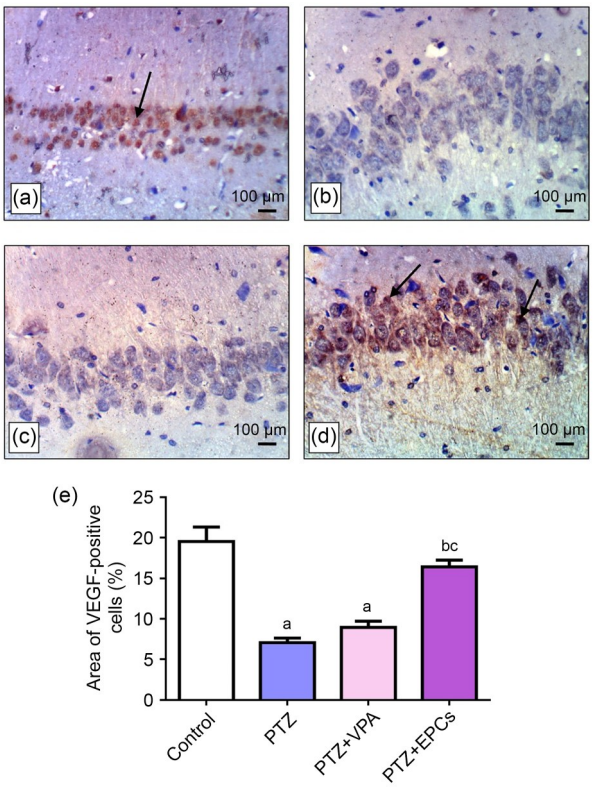

Fig. 5 Effects of EPCs on PTZ-induced alterations in immunohistochemically detected expression of hippocampal VEGF. Immunohistochemical staining: control group (a), PTZ group (b), PTZ+VPA group (c), and PTZ+EPC group (d). The arrows highlight the immunostained area (brown). (e) Area percentage of VEGF-positive cells. The data were analyzed using one-way ANOVA followed by the Tukey-Kramer test. Each column with a vertical line represents the mean±SEM (n=10). [a] Significantly different from the control group; [b] Significantly different from the PTZ group; [c] Significantly different from the PTZ+VPA group. P<0.05 is considered to indicate statistical significance. ANOVA: analysis of variance; EPCs: endothelial progenitor cells; PTZ: pentylenetetrazole; SEM: standard error of the mean; VEGF: vascular endothelial growth factor; VPA: valproic acid.

damage caused by seizures can result in cognitive impairment (Safar et al., 2020; Khalife et al., 2022). Findings from our earlier report confirmed the characterization of EPCs through the surface expression of CD31, CD34, and CD133 markers using flow cytometry, with percentages of expression of 30%, 65%, and 36%, respectively. The migration of EPCs to the hippocampus of PTZ-kindled rats has also been established through fluorescence imaging, which revealed labeled EPCs in the brains of epileptic animals, confirming their successful hippocampal homing (Ali et al., 2019).

The epileptic animals in the present investigation show memory and behavioral disruptions compared with the control animals, as proven by undermined activity in the OFT and the Y-maze test. These findings corroborate previous research that linked the PTZ-induced kindling phase to behavioral alterations and long-term memory impairments (Takechi et al., 2012; Pahwa and Goel, 2016). Promisingly, the administration of EPCs appears to have beneficial effects in terms of controlling seizure severity and reducing behavioral disturbances. This positive behavioral effect of EPCs is superior to that of many AEDs, such as phenytoin and VPA, which have no significant effects on locomotion or exploratory behaviors (Onuma, 2011; Aboeisa et al., 2022).

The largest number and highest proportion of tissue-specific lncRNAs are found in the brain (Aprea and Calegari, 2015). These brain-specific lncRNAs exhibit the greatest evolutionary conservation among all lncRNAs (Wang et al., 2016; Fernandes et al., 2018). In the present study, we found that PTZ significantly suppresses the hippocampal expression levels of the lncRNAs *Evf2*, *Pnky*, *Dlx1*, *APF*, *HOTAIR*, and *FLJ11812*, which are highly implicated in the regulation of both central nervous system (CNS) development and autophagy.

LncRNA *Dlx1* knockdown results in a reduction in *Dlx1*/*Dlx2* expression (Cobos et al., 2005), and *Dlx1*/*Dlx2* is crucial for determining the identity of neurons. Specifically, in the forebrain, *Dlx1*, *Dlx2*, *Dlx5*, and *Dlx6* all have important functions in guiding the tangential migration of GABAergic progenitors from the ventral telencephalon to their final termini, such as the neocortex and the striatum (Hoshino et al., 2021). In the same context, *Dlx1* has been implicated in murine behavioral aberrations, including hyperactivity, a reduced fear response, and epilepsy (Le et al., 2017; Lucchese and Stahl, 2018). The lncRNA *Evf2* is vital for GABAergic interneuron development (Bond et al., 2009) and adult brain circuitry (Kohtz, 2014; Hosseini et al., 2019). Consequently, its deletion is reported to cause seizures, hyperexcitability, and epilepsy (Jones et al., 2011). Our correlation analysis reveals a positive correlation between the two lncRNAs *Dlx1* and *Evf2*. Cajigas et al. (2015) discovered that *Evf2* can regulate gene expression and chromatin remodeling in the developing mouse forebrain via the formation of an *Evf2*-*Dlx1* ribonucleoprotein. *Evf2* plays a crucial role in regulating brain

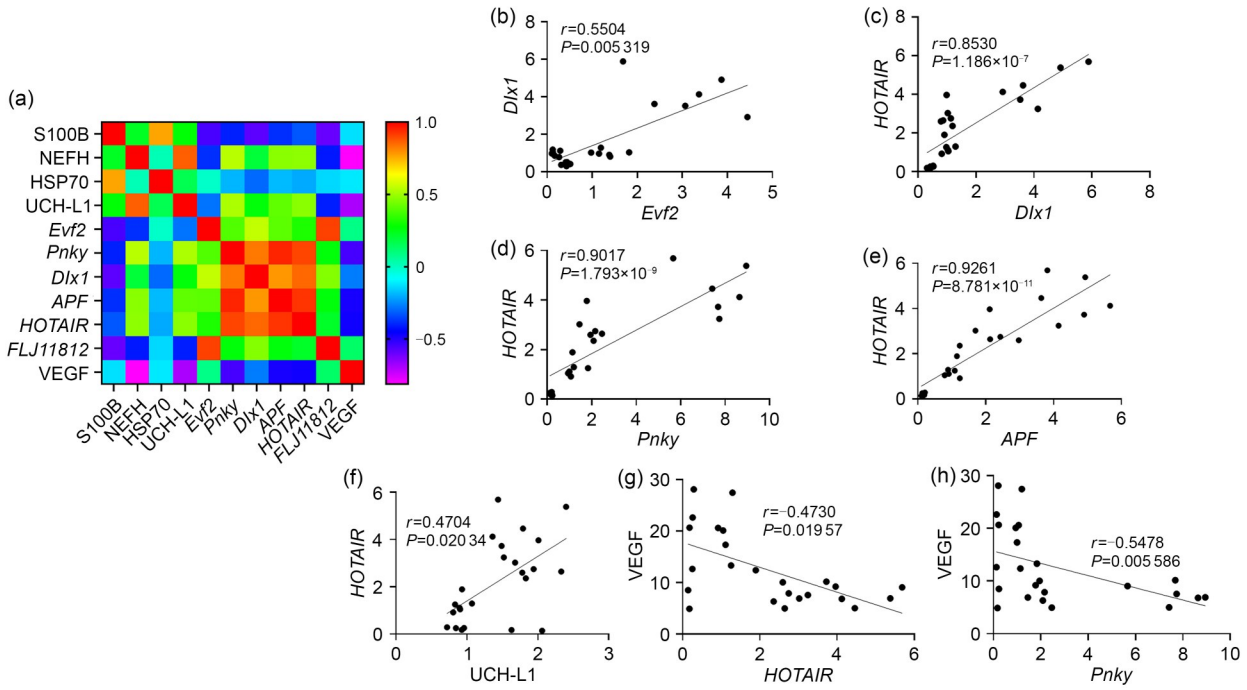

Fig. 6 Heatmap of correlations, linear regression, and representative correlation analyses. (a) Heatmap of Spearman's correlation matrix; (b) Correlation of the lncRNA *Dlx1* with the lncRNA *Evf2*; (c) Correlation of the lncRNA *Dlx1* with the lncRNA *HOTAIR*; (d) Correlation of the lncRNA *HOTAIR* with the lncRNA *Pnky*; (e) Correlation of the lncRNA *HOTAIR* with the lncRNA *APF*; (f) Correlation of the lncRNA *HOTAIR* with UCH-L1; (g) Correlation of VEGF with the lncRNA *HOTAIR*; (h) Correlation of VEGF with the lncRNA *Pnky*. Spearman's correlation coefficient (*r*) is shown. In the heatmap, parameters are clustered using Spearman's correlation as the distance metric. HSP70: heat shock protein 70; LncRNA: long noncoding RNA; NEFH: neurofilament heavy chain protein; S100B: soluble protein-100B; UCH-L1: ubiquitin carboxy-terminal hydrolase L1; VEGF: vascular endothelial growth factor.

development in humans by forming a complex with *Dlx1* and *Dlx2*. This complex promotes the enhancer activity of *Dlx5* and *Dlx6*, which is also necessary for brain development (Zhao and Li, 2022). Moreover, the expression profiles of *Evf1*/*Evf2* and their associated coding genes *Dlx5*/*Dlx6* and *Dlx1*/*Dlx2* are consistent (Fico et al., 2019).

Interestingly, the *Dlx1* gene is located adjacent to the *HOXD* gene cluster, indicating that the histone modifications induced by *HOTAIR* can potentially affect multiple genes located close to each other on the same chromosome. Contrary to the findings of Kuo et al. (2022), who reported that the *Dlx1* gene is epigenetically repressed by *HOTAIR* in their papillary thyroid cancer cell system, this study reveals a positive correlation between the expression of the lncRNAs *Dlx1* and *HOTAIR*.

Aprea and Calegari (2015) found that neuron production from neural stem cells is regulated by the conserved, neural-specific lncRNA *Pnky*. The regulation of neurogenesis in embryonic and postnatal neural stem cell populations involves interactions between the splicing regulator, polypyrimidine tract-binding protein 1 (PTBP1), and *Pnky*. *Pnky* knockdown depletes the neural stem cell population (Ramos et al., 2015). Accordingly, in dividing neural stem cells, *Pnky* controls the delicate balance between self-renewal and differentiation (Hines, 2016; Ilieva and Uchida, 2022). In line with the reported ability of *HOTAIR* to bind to PTBP1 (Tello-Flores et al., 2021; Tan et al., 2022), our findings reveal a positive correlation between *Pnky* and *HOTAIR*.

The lncRNA *FLJ11812* can act as a sponge for miR-4488, miR-3960, and miR-4459, thus upregulating their targets, including autophagy-related protein-13 (ATG-13) (Gao et al., 2016). This link helps to clarify the alterations in autophagy detected with the corresponding variations in the *FLJ11812* level (Ge et al., 2014). Essentially, *HOTAIR* contributes to the activation of autophagy through the upregulation of ATG-3 and ATG-7 at both the transcriptional and translational levels (Zhang et al., 2021; Wang JL et al.,

2022). The lncRNA *APF* is upregulated to protect ATG-7 from being downregulated by miR-188-3p. Despite poor conservation of the full-length *APF* across species, the binding site for miR-188-3p is highly conserved, which underscores the importance of the *APF*/miR-188-3p/ATG-7 regulatory pathway in promoting autophagy (Wang et al., 2015; Zeng et al., 2022). Similarly, through the miR-874-5p/ATG-10 axis, *HOTAIR* increases autophagy and inhibits apoptosis (Zhao et al., 2020; Gupta et al., 2021). The positive correlation between *HOTAIR* and *APF* detected in the present study is comprehensible in light of the positive regulatory roles of both lncRNAs in autophagy.

In this study, the administration of PTZ significantly increased plasma levels of S100B, NEFH, HSP70, and UCH-L1 compared to those in control animals. Early after seizures, the S100B protein can be utilized as a biochemical marker to evaluate brain damage (Liang et al., 2019; Seçen et al., 2023), because it indicates BBB damage and impaired astrocyte function in rats with chronic seizures. Based on the high inducibility of HSP70, it can presumably be synthesized after an insult as a neuroprotective protein (Rejdak et al., 2012; Kim et al., 2020). UCH-L1 is a protein that is present in significant amounts in the mammalian brain and plays a vital role in hippocampal synaptic function (Matuszczak et al., 2020). Due to its clinically important attributes and high brain specificity, UCH-L1 is a potential biomarker for neuronal damage and BBB disruption (Mondello et al., 2012; Öhrfelt et al., 2016). As a signaling molecule, UCH-L1 may coordinate the effects of the autophagy–lysosome pathway, which mediates the degradation of protein aggregates in the cytoplasm (Yu et al., 2018). UCH-L1 physically interacts with HSP70 and HSP90 and is intricately involved in the monitoring mechanism of the chaperone-mediated autophagy pathway (Kanno et al., 2022). This positive regulatory role of UCH-L1 in autophagy may explain the positive correlation observed here between UCH-L1 and *HOTAIR*.

Equally important, NEFH is the most widely phosphorylated protein in the human brain, with modulatory effects on axonal transport and cell-structure homeostasis. NEFH, a biomarker of axonal damage, has correspondingly emerged as a biomarker of neurodegeneration (Rejdak et al., 2012; Xin et al., 2023). Overall, we hypothesize that increased plasma levels of S100B, NEFH, HSP70, and UCH-L1 indicate significant neuronal and BBB damages in the PTZ-induced kindling model. Interestingly, the administration of EPCs resulted in a significant reduction in the plasma levels of these neuronal damage markers compared with those in epileptic rats, confirming the great regenerative properties of these cells.

We found reduced VEGF expression in the hippocampus of epileptic rats, as detected by immunohistochemistry. The expression of VEGF is controlled by neuronal and glial cells following seizures in the hippocampus of epileptic rodents, indicating that it has a neuroprotective role (Ogaki et al., 2020). EPCs produce growth factors, such as VEGF, that enhance neuronal survival (Chang et al., 2013; Park et al., 2014). The present findings show that the administration of EPCs to epileptic rats significantly increases VEGF levels, demonstrating that EPCs can have a paracrine effect by supplying neurotrophic factors to the epileptic brain. The data in this study reveal strong negative correlations between VEGF and the lncRNAs *HOTAIR* and *Pnky*. These results corroborate those reported by both Biswas et al. (2021) and Wu et al. (2019), who reported that *HOTAIR* regulates VEGF through the binding of histone-modifying enzymes. VEGF mRNA levels are inversely linked to *HOTAIR* levels in diabetic retinopathy (Biswas et al., 2021). *HOTAIR* has also been found to repress placental angiogenesis by hindering VEGF expression in human placental tissue (Wu et al., 2019). Similarly, through binding to PTBP1, *Pnky* can regulate the function of VEGF in choroidal neovascularization lesions. *Pnky* silencing can affect the regulatory function of VEGF and its endothelial angiogenic effects in endothelial cells both in vitro and in vivo (Shi et al., 2022).

In the present study, the mRNA expression of the studied lncRNAs significantly increased after treatment with EPCs. The therapeutic efficacy of stem cell treatment could directly depend on stem cell homing and transdifferentiation, or more likely, on a paracrine mode of action, in which stem cells release protective soluble factors to neighboring cells (Avolio et al., 2015; Qin et al., 2022). The paracrine mechanism of action of newly emerged stem cells involves the release of certain intracellular constituents (mainly proteins and mRNAs) along with selected patterns of mature microRNAs and lncRNAs via specific vesicles called exosomes (Li et al., 2018; Guy and Offen, 2020; Xie et al., 2020; Feng et al., 2022; He et al., 2022; Wang SS et al., 2022; Wu et al., 2022; Wang

HM et al., 2023). The transfer of such materials via exosomes induces phenotypic and functional alterations in recipient cells. Thus, stem cells may execute and regulate their biological outcomes by conveying genetic information and modulating target-cell gene expression via exosome-mediated mRNA, microRNA, and lncRNA delivery (Ratajczak and Ratajczak, 2016; Li et al., 2018; Wang SS et al., 2022). Stem cell-derived exosomes may likewise stimulate epigenetic alterations in target cells (Ratajczak et al., 2006, 2016). In view of this, it can be assumed that the observed effect of EPCs on the studied lncRNAs is mediated through the biological activity of stem cell-derived exosomes.

5 Conclusions

Our study provides new insights into the antiepileptic effects of EPCs in PTZ-induced seizures. EPC treatment is superior to VPA treatment in terms of its impact on seizure severity, behavioral changes, neuronal damage, neurotrophic factors, and relevant lncRNAs. EPCs have the potential to be used in antiepileptic treatment and can act through a combination of several biological effects that may include the upregulation of specific regulatory lncRNAs. Promising interventions for neurodegenerative diseases and acute CNS neurological insults could potentially be developed through the modulation of the lncRNAs involved in brain development and autophagy machinery. Despite this potential, this area of research has not been thoroughly explored. Thus, it is important to conduct additional research to gain a better understanding of the role that stem cells play in different pathophysiological brain processes. Elucidating the modulatory potential of EPCs for lncRNAs may also be a fruitful avenue for developing more targeted antiepileptic therapeutic interventions.

Data availability statement

The majority of the data are available within the paper and its supplementary file. Should any raw data files be needed, they are available from the corresponding author upon reasonable request.

Acknowledgments

Funding note: Open access funding provided by The Science, Technology & Innovation Funding Authority (STDF) in cooperation with The Egyptian Knowledge Bank (EKB).

Author contributions

Shimaa O. ALI: conceptualization, investigation, data curation, validation, formal analysis, writing – original draft, and writing – review and editing. Nancy N. SHAHIN: conceptualization, validation, and writing – review and editing. Marwa M. SAFAR: conceptualization, methodology, and writing – review and editing. Sherine M. RIZK: conceptualization, supervision, and writing – review and editing. All authors have read and approved the final manuscript, and therefore, have full access to all the data in the study and take responsibility for the integrity and security of the data.

Compliance with ethics guidelines

Shimaa O. ALI, Nancy N. SHAHIN, Marwa M. SAFAR, and Sherine M. RIZK declare that they have no conflicts of interest.

All the procedures followed for handling the animals were in accordance with the Helsinki Declaration of 1975, as revised in 2008(5) concerning animal rights. The Research Ethics Committee of the Faculty of Pharmacy, Cairo University (REC-FOPCU) approved this study under approval number BC 1838. All institutional and national guidelines for the care and use of laboratory animals were followed.

References

Aboeisa MI, Seleem MAH, el Gohary TM, et al., 2022. Study of cognitive and behavioral impacts of idiopathic epilepsy and antiepileptic drugs (AEDs) in children and adolescents. *J Adv Med Med Res*, 34(19):176-187. https://doi.org/10.9734/jammr/2022/v34i1931451

Ali SO, Shahin NN, Safar MM, et al., 2019. Therapeutic potential of endothelial progenitor cells in a rat model of epilepsy: role of autophagy. *J Adv Res*, 18:101-112. https://doi.org/10.1016/j.jare.2019.01.013

Aprea J, Calegari F, 2015. Long non-coding RNAs in corticogenesis: deciphering the non-coding code of the brain. *EMBO J*, 34(23):2865-2884. https://doi.org/10.15252/embj.201592655

Avolio E, Caputo M, Madeddu P, 2015. Stem cell therapy and tissue engineering for correction of congenital heart disease. *Front Cell Dev Biol*, 3:39. https://doi.org/10.3389/fcell.2015.00039

Biswas S, Feng B, Chen SL, et al., 2021. The long non-coding RNA *HOTAIR* is a critical epigenetic mediator of angiogenesis in diabetic retinopathy. *Invest Ophthalmol Vis Sci*, 62(3):20.

https://doi.org/10.1167/iovs.62.3.20

Bond AM, Vangompel MJW, Sametsky EA, et al., 2009. Balanced gene regulation by an embryonic brain ncRNA is critical for adult hippocampal GABA circuitry. *Nat Neurosci*, 12(8):1020-1027. https://doi.org/10.1038/nn.2371

Cajigas I, Leib DE, Cochrane J, et al., 2015. *Evf2* lncRNA/BRG1/DLX1 interactions reveal RNA-dependent inhibition of chromatin remodeling. *Development*, 142(15):2641-2652. https://doi.org/10.1242/dev.126318

Chang JL, Atochin DN, Li Q, et al., 2013. Bone marrow-derived circulating endothelial progenitor cells contribute to ENOS-regulated endothelial repair and vasodilation after arterial injury in vivo. *J Cardio Vasc Med*, 1:1-8.

Cobos I, Calcagnotto ME, Vilaythong AJ, et al., 2005. Mice lacking *Dlx1* show subtype-specific loss of interneurons, reduced inhibition and epilepsy. *Nat Neurosci*, 8(8):1059-1068. https://doi.org/10.1038/nn1499

Croce N, Mathé AA, Gelfo F, et al., 2014. Effects of lithium and valproic acid on BDNF protein and gene expression in an *in vitro* human neuron-like model of degeneration. *J Psychopharmacol*, 28(10):964-972. https://doi.org/10.1177/0269881114529379

Cuevas-Diaz Duran R, Wei H, Kim DH, et al., 2019. Invited Review: long non-coding RNAs: important regulators in the development, function and disorders of the central nervous system. *Neuropathol Appl Neurobiol*, 45(6):538-556. https://doi.org/10.1111/nan.12541

Dhir A, 2012. Pentylenetetrazol (PTZ) kindling model of epilepsy. *Curr Protoc Neurosci*, 58:9.37.1-9.37.12. https://doi.org/10.1002/0471142301.ns0937s58

Dunn C, Sturdivant N, Venier S, et al., 2021. Blood–brain barrier breakdown and astrocyte reactivity evident in the absence of behavioral changes after repeated traumatic brain injury. *Neurotrauma Rep*, 2(1):399-410. https://doi.org/10.1089/neur.2021.0017

Erkeç ÖE, 2015. Pentylenetetrazol kindling epilepsy model. *J Turkish Epilepsi Soc*, 21(1):6-12. https://doi.org/10.5505/epilepsi.2015.08108

Feng ZY, Zhang QY, Tan J, et al., 2022. Techniques for increasing the yield of stem cell-derived exosomes: what factors may be involved? *Sci China Life Sci*, 65(7):1325-1341. https://doi.org/10.1007/s11427-021-1997-2

Fernandes DP, Bitar M, Jacobs FMJ, et al., 2018. Long noncoding RNAs in neuronal aging. *Noncoding RNA*, 4(2):12. https://doi.org/10.3390/ncrna4020012

Fernandes JCR, Acuña SM, Aoki JI, et al., 2019. Long noncoding RNAs in the regulation of gene expression: physiology and disease. *Noncoding RNA*, 5(1):17. https://doi.org/10.3390/ncrna5010017

Fico A, Fiorenzano A, Pascale E, et al., 2019. Long non-coding RNA in stem cell pluripotency and lineage commitment: functions and evolutionary conservation. *Cell Mol Life Sci*, 76(8):1459-1471. https://doi.org/10.1007/s00018-018-3000-z

Gao J, Jiao H, Cao R, et al., 2016. In vitro study of effects and mechanism of rapamycin-induced autophagy in keloid fibroblasts. *Chin J Plast Surg*, 32(3):208-214 (in Chinese). https://doi.org/10.3760/cma.j.issn.1009-4598.2016.03.012

Ge D, Han L, Huang SY, et al., 2014. Identification of a novel MTOR activator and discovery of a competing endogenous RNA regulating autophagy in vascular endothelial cells. *Autophagy*, 10(6):957-971. https://doi.org/10.4161/auto.28363

Ghafouri S, Fathollahi Y, Javan M, et al., 2016. Effect of low frequency stimulation on impaired spontaneous alternation behavior of kindled rats in Y-maze test. *Epilepsy Res*, 126:37-44. https://doi.org/10.1016/j.eplepsyres.2016.06.010

Gu P, Xu ZH, Cao YZ, et al., 2020. Synchrotron radiation-based three-dimensional visualization of angioarchitectural remodeling in hippocampus of epileptic rats. *Neurosci Bull*, 36(4):333-345. https://doi.org/10.1007/s12264-019-00450-0

Gupta R, Ambasta RK, Kumar P, 2021. Autophagy and apoptosis cascade: which is more prominent in neuronal death? *Cell Mol Life Sci*, 78(24):8001-8047. https://doi.org/10.1007/s00018-021-04004-4

Guy R, Offen D, 2020. Promising opportunities for treating neurodegenerative diseases with mesenchymal stem cell-derived exosomes. *Biomolecules*, 10(9):1320. https://doi.org/10.3390/biom10091320

He LL, Lin MM, Shen J, et al., 2022. Emerging role of exosomal long non-coding RNAs in lung cancer. *Mol Biol Rep*, 49(6):4989-4997. https://doi.org/10.1007/s11033-022-07169-8

Hines PJ, 2016. A long noncoding RNA for neuronal differentiation. *Science*, 353(6297):360-361. https://doi.org/10.1126/science.353.6297.360-d

Hogan RE, 2018. Drug resistant epilepsy and new AEDs: two perspectives. *Epilepsy Curr*, 18(5):304-306. https://doi.org/10.5698/1535-7597.18.5.304

Hoshino C, Konno A, Hosoi N, et al., 2021. GABAergic neuron-specific whole-brain transduction by AAV-PHP.B incorporated with a new GAD65 promoter. *Mol Brain*, 14:33. https://doi.org/10.1186/s13041-021-00746-1

Hosseini E, Bagheri-Hosseinabadi Z, de Toma I, et al., 2019. The importance of long non-coding RNAs in neuropsychiatric disorders. *Mol Aspects Med*, 70:127-140. https://doi.org/10.1016/j.mam.2019.07.004

Ilieva M, Uchida S, 2022. Long noncoding RNAs in induced pluripotent stem cells and their differentiation. *Am J Physiol Cell Physiol*, 322(4):C769-C774. https://doi.org/10.1152/ajpcell.00059.2022

Jones DL, Howard MA, Stanco A, et al., 2011. Deletion of *Dlx1* results in reduced glutamatergic input to hippocampal interneurons. *J Neurophysiol*, 105(5):1984-1991.

https://doi.org/10.1152/jn.00056.2011

Kanno H, Handa K, Murakami T, et al., 2022. Chaperone-mediated autophagy in neurodegenerative diseases and acute neurological insults in the central nervous system. *Cells*, 11(7):1205. https://doi.org/10.3390/CELLS11071205

Khalife MR, Scott RC, Hernan AE, 2022. Mechanisms for cognitive impairment in epilepsy: moving beyond seizures. *Front Neurol*, 13:878991. https://doi.org/10.3389/fneur.2022.878991

Kim CK, Park JS, Kim E, et al., 2022. The effects of early exercise in traumatic brain-injured rats with changes in motor ability, brain tissue, and biomarkers. *BMB Rep*, 55(10): 512-517. https://doi.org/10.5483/BMBRep.2022.55.10.097

Kim JY, Barua S, Huang MY, et al., 2020. Heat shock protein 70 (HSP70) induction: chaperonotherapy for neuroprotection after brain injury. *Cells*, 9(9):2020. https://doi.org/10.3390/cells9092020

Kobayashi K, Endoh F, Ohmori I, et al., 2020. Action of antiepileptic drugs on neurons. *Brain Dev*, 42(1):2-5. https://doi.org/10.1016/j.braindev.2019.07.006

Kohtz JD, 2014. Long non-coding RNAs learn the importance of being *in vivo*. *Front Genet*, 5:45. https://doi.org/10.3389/fgene.2014.00045

Kuo FC, Wang YT, Liu CH, et al., 2022. LncRNA *HOTAIR* impairs the prognosis of papillary thyroid cancer via regulating cellular malignancy and epigenetically suppressing *DLX1*. *Cancer Cell Int*, 22:396. https://doi.org/10.1186/s12935-022-02817-2

Le TN, Zhou QP, Cobos I, et al., 2017. GABAergic interneuron differentiation in the basal forebrain is mediated through direct regulation of glutamic acid decarboxylase isoforms by *Dlx* homeobox transcription factors. *J Neurosci*, 37(36): 8816-8829. https://doi.org/10.1523/JNEUROSCI.2125-16.2017

Li L, Luo Q, Shang B, et al., 2022. Selective activation of cannabinoid receptor-2 reduces white matter injury via PERK signaling in a rat model of traumatic brain injury. *Exp Neurol*, 347:113899. https://doi.org/10.1016/j.expneurol.2021.113899

Li P, Jia YY, Tang WB, et al., 2021. Roles of non-coding RNAs in central nervous system axon regeneration. *Front Neurosci*, 15:630633. https://doi.org/10.3389/fnins.2021.630633

Li SL, Li YC, Chen B, et al., 2018. ExoRBase: a database of circRNA, lncRNA and mRNA in human blood exosomes. *Nucleic Acids Res*, 46(D1):D106-D112. https://doi.org/10.1093/nar/gkx891

Liang KG, Mu RZ, Liu Y, et al., 2019. Increased serum S100B levels in patients with epilepsy: a systematic review and meta-analysis study. *Front Neurosci*, 13:456. https://doi.org/10.3389/fnins.2019.00456

Lucchese G, Stahl B, 2018. Peptide sharing between viruses and DLX proteins: a potential cross-reactivity pathway to neuropsychiatric disorders. *Front Neurosci*, 12:150. https://doi.org/10.3389/fnins.2018.00150

Ma QQ, Long SH, Gan ZD, et al., 2022. Transcriptional and post-transcriptional regulation of autophagy. *Cells*, 11(3): 441. https://doi.org/10.3390/cells11030441

Marchi N, Lerner-Natoli M, 2013. Cerebrovascular remodeling and epilepsy. *Neuroscientist*, 19(3):304-312. https://doi.org/10.1177/1073858412462747

Matuszczak E, Tylicka M, Komarowska MD, et al., 2020. Ubiquitin carboxy-terminal hydrolase L1 – physiology and pathology. *Cell Biochem Funct*, 38(5):533-540. https://doi.org/10.1002/cbf.3527

Mondello S, Palmio J, Streeter J, et al., 2012. Ubiquitin Carboxy-Terminal Hydrolase L1 (UCH-L1) is increased in cerebrospinal fluid and plasma of patients after epileptic seizure. *BMC Neurol*, 12:85. https://doi.org/10.1186/1471-2377-12-85

Morin-Brureau M, Lebrun A, Rousset MC, et al., 2011. Epileptiform activity induces vascular remodeling and zonula occludens 1 downregulation in organotypic hippocampal cultures: role of VEGF signaling pathways. *J Neurosci*, 31(29):10677-10688. https://doi.org/10.1523/JNEUROSCI.5692-10.2011

Ogaki A, Ikegaya Y, Koyama R, 2020. Vascular abnormalities and the role of vascular endothelial growth factor in the epileptic brain. *Front Pharmacol*, 11:20. https://doi.org/10.3389/fphar.2020.00020

Öhrfelt A, Johansson P, Wallin A, et al., 2016. Increased cerebrospinal fluid levels of ubiquitin carboxyl-terminal hydrolase L1 in patients with Alzheimer's disease. *Dement Geriatr Cogn Dis Extra*, 6(2):283-294. https://doi.org/10.1159/000447239

Onuma T, 2011. Cognitive dysfunction and antiepileptic drugs. *Brain Nerve*, 63(4):379-383 (in Japanese). https://doi.org/10.11477/mf.1416100882

Pahwa P, Goel RK, 2016. Ameliorative effect of *Asparagus racemosus* root extract against pentylenetetrazol-induced kindling and associated depression and memory deficit. *Epilepsy Behav*, 57:196-201. https://doi.org/10.1016/j.yebeh.2016.01.025

Park KJ, Park E, Liu E, et al., 2014. Bone marrow-derived endothelial progenitor cells protect postischemic axons after traumatic brain injury. *J Cereb Blood Flow Metab*, 34(2): 357-366. https://doi.org/10.1038/jcbfm.2013.216

Qin C, Wang KW, Zhang L, et al., 2022. Stem cell therapy for Alzheimer's disease: an overview of experimental models and reality. *Anim Model Exp Med*, 5(1):15-26. https://doi.org/10.1002/ame2.12207

Racine RJ, 1972. Modification of seizure activity by electrical stimulation. II. Motor seizure. *Electroencephalogr Clin Neurophysiol*, 32(3):281-294. https://doi.org/10.1016/0013-4694(72)90177-0

Ramos AD, Andersen RE, Liu SJ, et al., 2015. The long noncoding RNA *Pnky* regulates neuronal differentiation of embryonic and postnatal neural stem cells. *Cell Stem*

Cell, 16(4):439-447. https://doi.org/10.1016/j.stem.2015.02.007

Ratajczak J, Miekus K, Kucia M, et al., 2006. Embryonic stem cell-derived microvesicles reprogram hematopoietic progenitors: evidence for horizontal transfer of mRNA and protein delivery. *Leukemia*, 20(5):847-856. https://doi.org/10.1038/sj.leu.2404132

Ratajczak MZ, Ratajczak J, 2016. Horizontal transfer of RNA and proteins between cells by extracellular microvesicles: 14 years later. *Clin Trans Med*, 5(1):e7. https://doi.org/10.1186/s40169-016-0087-4

Ratajczak MZ, Ratajczak D, Pedziwiatr D, 2016. Extracellular microvesicles (ExMVs) in cell to cell communication: a role of telocytes. *In*: Wang XD, Cretoiu D (Eds.), Telocytes. Springer, Singapore, p.41-49. https://doi.org/10.1007/978-981-10-1061-3_3

Rejdak K, Kuhle J, Rüegg S, et al., 2012. Neurofilament heavy chain and heat shock protein 70 as markers of seizure-related brain injury. *Epilepsia*, 53(5):922-927. https://doi.org/10.1111/j.1528-1167.2012.03459.x

Safar MM, Arab HH, Rizk SM, et al., 2016. Bone marrow-derived endothelial progenitor cells protect against scopolamine-induced Alzheimer-like pathological aberrations. *Mol Neurobiol*, 53(3):1403-1418. https://doi.org/10.1007/s12035-014-9051-8

Safar MM, Shahin NN, Mohamed AF, et al., 2020. Suppression of BACE1 and amyloidogenic/RAGE axis by sitagliptin ameliorates PTZ kindling-induced cognitive deficits in rats. *Chem Biol Interact*, 328:109144. https://doi.org/10.1016/j.cbi.2020.109144

Seçen AE, Akçalı DT, Kurt G, 2023. The S100B protein in epilepsy. *Arch Epilepsy*, 29(2):37-40. https://doi.org/10.4274/ArchEpilepsy.2023.231289

Shi LJ, Han X, Liu C, et al., 2022. Long non-coding RNA PNKY modulates the development of choroidal neovascularization. *Front Cell Dev Biol*, 10:836031. https://doi.org/10.3389/fcell.2022.836031

Takechi K, Suemaru K, Kawasaki H, et al., 2012. Impaired memory following repeated pentylenetetrazol treatments in kindled mice. *Yakugaku Zasshi*, 132(2):179-182 (in Japanese). https://doi.org/10.1248/yakushi.132.179

Tan W, Wang K, Yang X, et al., 2022. LncRNA HOTAIR promotes myocardial fibrosis in atrial fibrillation through binding with PTBP1 to increase the stability of Wnt5a. *Int J Cardiol*, 369:21-28. https://doi.org/10.1016/j.ijcard.2022.06.073

Tello-Flores VA, Beltrán-Anaya FO, Ramírez-Vargas MA, et al., 2021. Role of long non-coding RNAs and the molecular mechanisms involved in insulin resistance. *Int J Mol Sci*, 22(14):7256. https://doi.org/10.3390/ijms22147256

van Vliet EA, Ndode-Ekane XE, Lehto LJ, et al., 2020. Long-lasting blood-brain barrier dysfunction and neuroinflammation after traumatic brain injury. *Neurobiol Dis*, 145:105080. https://doi.org/10.1016/j.nbd.2020.105080

Wang HM, Huber CC, Li XP, 2023. Mesenchymal and neural stem cell-derived exosomes in treating Alzheimer's disease. *Bioengineering*, 10(2):253. https://doi.org/10.3390/BIOENGINEERING10020253

Wang JL, Zhao JH, Hu P, et al., 2022. Long non-coding RNA HOTAIR in central nervous system disorders: new insights in pathogenesis, diagnosis, and therapeutic potential. *Front Mol Neurosci*, 15:949095. https://doi.org/10.3389/fnmol.2022.949095

Wang K, Liu CY, Zhou LY, et al., 2015. APF lncRNA regulates autophagy and myocardial infarction by targeting miR-188-3p. *Nat Commun*, 6:6779. https://doi.org/10.1038/ncomms7779

Wang L, Liu Y, Sun SQ, et al., 2016. Regulation of neuronal-glial fate specification by long non-coding RNAs. *Rev Neurosci*, 27(5):491-499. https://doi.org/10.1515/revneuro-2015-0061

Wang PH, Chen W, Zhao S, et al., 2023. The role of LncRNA-regulated autophagy in AKI. *BioFactors*, 49(5):1010-1021. https://doi.org/10.1002/biof.1980

Wang SS, Xu LJ, Zhu KL, et al., 2022. Developing and validating a survival prediction model based on blood exosomal ceRNA network in patients with PAAD. *BMC Med Genomics*, 15:260. https://doi.org/10.1186/s12920-022-01409-3

Wu KJ, Liu FL, Wu WR, et al., 2019. Long non-coding RNA *HOX* transcript antisense RNA (*HOTAIR*) suppresses the angiogenesis of human placentation by inhibiting vascular endothelial growth factor A expression. *Reprod Fertil Dev*, 31(2):377-385. https://doi.org/10.1071/RD18118

Wu XM, Bian B, Lin ZF, et al., 2022. Identification of exosomal mRNA, lncRNA and circRNA signatures in an osteoarthritis synovial fluid-exosomal study. *Exp Cell Res*, 410(1):112881. https://doi.org/10.1016/j.yexcr.2021.112881

Xie F, Liu YL, Chen XY, et al., 2020. Role of microRNA, lncRNA, and exosomes in the progression of osteoarthritis: a review of recent literature. *Orthop Surg*, 12(3):708-716. https://doi.org/10.1111/os.12690

Xin YB, Lin GJ, Hua TB, et al., 2023. The altered expression of cytoskeletal and synaptic remodeling proteins during epilepsy. *Open Life Sci*, 18(1):20220595. https://doi.org/10.1515/biol-2022-0595

Yamanaka G, Takata F, Kataoka Y, et al., 2021. The neuroinflammatory role of pericytes in epilepsy. *Biomedicines*, 9(7):759. https://doi.org/10.3390/BIOMEDICINES9070759

Yu QT, Zhang HM, Li Y, et al., 2018. UCH-L1 inhibition suppresses tau aggresome formation during proteasomal impairment. *Mol Neurobiol*, 55(5):3812-3821. https://doi.org/10.1007/s12035-017-0558-7

Zeng HT, Hu FX, Duan Y, et al., 2022. Expression of lncRNA APF in peripheral blood of patients with acute myocardial infarction caused by coronary heart disease and its clinical

significance. *Int Heart J*, 63(4):742-748. https://doi.org/10.1536/ihj.21-434

Zhang JY, Chen K, Tang YX, et al., 2021. LncRNA-HOTAIR activates autophagy and promotes the imatinib resistance of gastrointestinal stromal tumor cells through a mechanism involving the miR-130a/*ATG2B* pathway. *Cell Death Dis*, 12(4):367. https://doi.org/10.1038/s41419-021-03650-7

Zhang PJ, Wu WY, Chen Q, et al., 2019. Non-coding RNAs and their integrated networks. *J Integr Bioinform*, 16(3): 20190027. https://doi.org/10.1515/jib-2019-0027

Zhao JY, Li HL, Chang N, 2020. LncRNA hotair promotes MPP^+-induced neuronal injury in Parkinson's disease by regulating the miR-874-5p/ATG10 axis. *EXCLI J*, 19:1141-1153. https://doi.org/10.17179/excli2020-2286

Zhao YY, Li P, 2022. Strategies of lncRNA DLX6-AS1 on study and therapeutics. *Front Genet*, 13:871988. https://doi.org/10.3389/fgene.2022.871988

Zimcikova E, Simko J, Karesova I, et al., 2017. Behavioral effects of antiepileptic drugs in rats: are the effects on mood and behavior detectable in open-field test? *Seizure*, 52:35-40. https://doi.org/10.1016/j.seizure.2017.09.015

Supplementary information

Table S1